Electronic Supplementary Material (ESI) for Physical Chemistry Chemical Physics.

Supporting Information

Photoinduced ICT vs Excited Rotamer Intercoversion in two quadrupolar polyaromatic N-methylpyridinium cations.

A. Cesaretti, B. Carlotti, F. Elisei, C. G. Fortuna and A. Spalletti

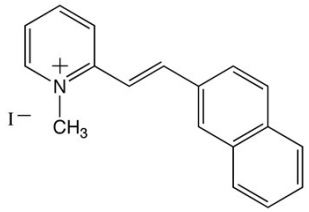

[**N1**]

1-methyl-2-[(*E*)-2-(2-naphthyl)vinyl]pyridinium

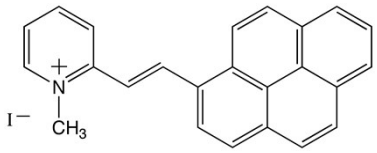

[**P1**]

1-methyl-2-[(*E*)-2-(1-pyrenyl)vinyl]pyridinium

Chart S1. Dipolar congeners of the investigated compounds.

Spectral, photophysical and photochemical properties

Table S1. Full Width at Half Maximum (FWHM) of the absorption and emission bands of **N1** and **N2** in solvents of different polarity and/or viscosity.

Solvent	FWHM /cm^{-1}			
	Absorption		Emission	
	N1*	N2	N1*	N2
DCM	6100	4500	3300	3200
DCE	6000	4300	3300	3200
2-PrOH	5500	4500	3800	3400
EtOH	5700	4400	3700	3500
MeOH	5700	4600	3800	3600
MeCN	5900	4600	3600	3600
MeOH/Gly (70/30)	-	4300	-	3600
MeOH/Gly (50/50)	5400	4600	3800	3600
EtGly	5800	4500	3700	3700
W/EtOH (70/30)	5800	5100	3600	4000

*From ref. 39.

Table S2. Full Width at Half Maximum (FWHM) of the absorption and emission bands of **P2** in solvents of different polarity and/or viscosity.

Solvent	FWHM /cm^{-1}	
	Absorption	Emission
DCM	3900	2800
DCE	4100	2900
2-PrOH	4300	3000
EtOH	4300	3200
MeOH/Gly (70/30)	4400	3300
MeOH	4500	3400
Ac	4600	3300

MeCN	4600	3500
EtGly	4600	3200

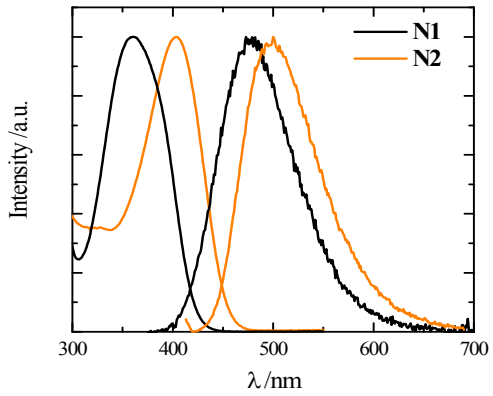

Figure S1. Normalized absorption and emission spectra of **N1** (black) and **N2** (orange) in 2-PrOH.

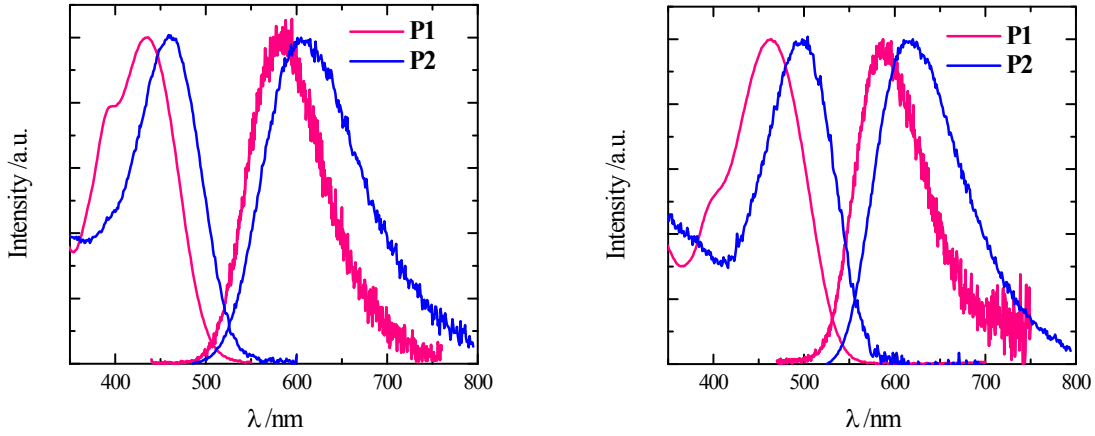

Figure S2. Normalized absorption and emission spectra of **P1** (pink) and **P2** (blu) in MeOH, left graph and DCM, right graph.

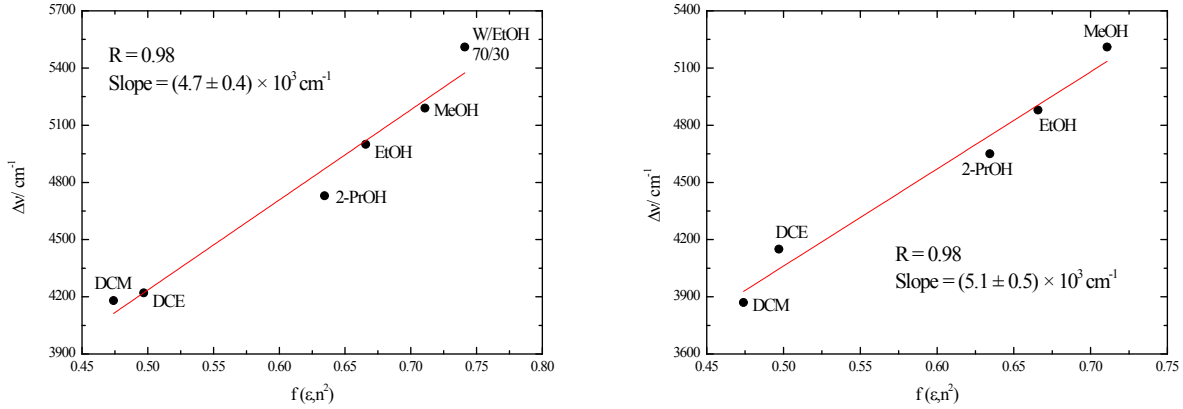

Figure S3. Quantification of the negative solvatochromism of **N2**, left graph, and **P2**, right graph, by the plot of the Stokes shift (Δν) as a function of the polarity parameter f(ε,n²), according to eq.1.

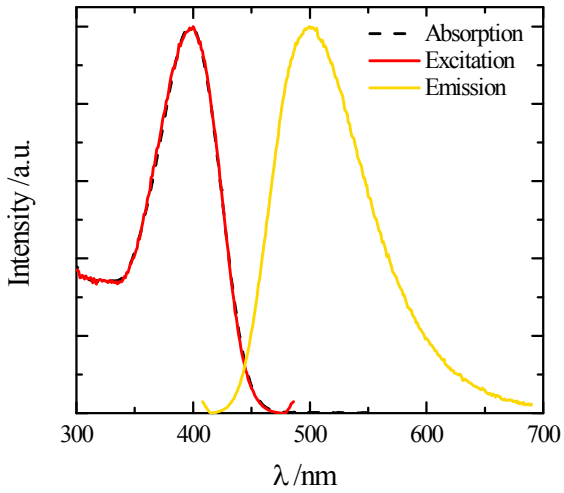

Figure S4. Absorption (black dashed line), excitation (red) and emission (yellow) spectra of **N2** in MeOH.

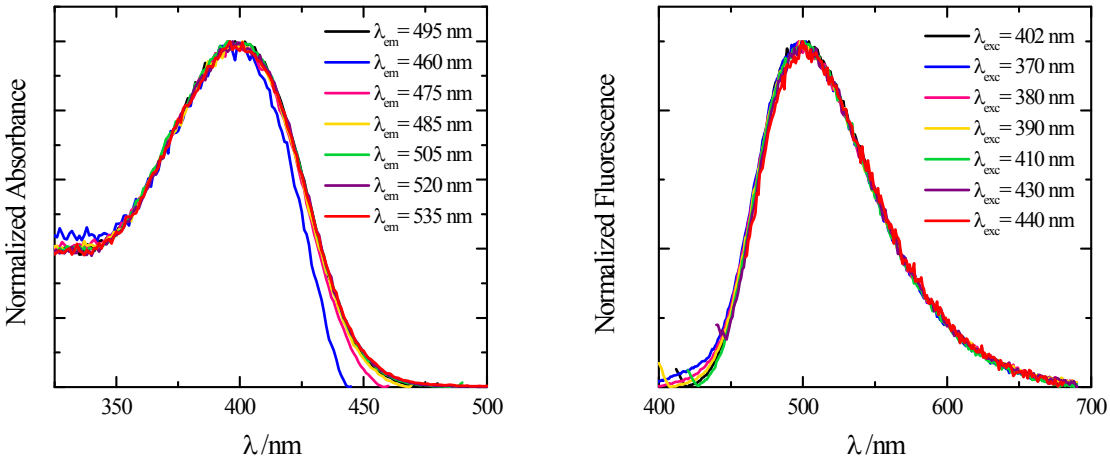

Figure S5. Emission wavelength effect on the excitation spectrum (left graph) and excitation wavelength effect on the emission spectrum (right graph) for **N2** in MeOH/Gly 50/50.

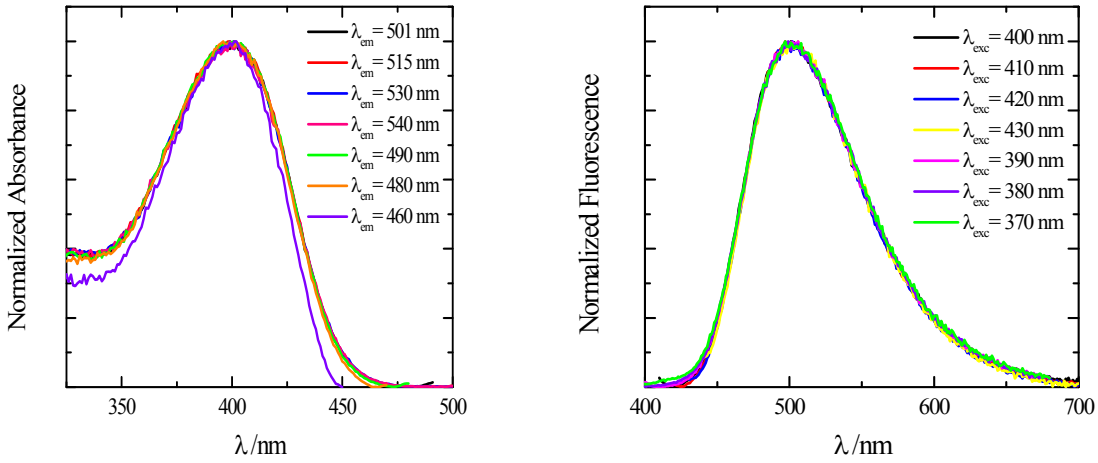

Figure S6. Emission wavelength effect on the excitation spectrum (left graph) and excitation wavelength effect on the emission spectrum (right graph) for **N2** in EtGly.

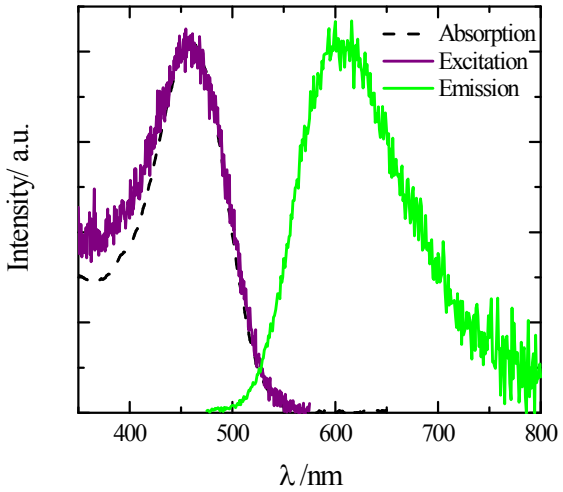

Figure S7. Absorption (black dashed line), excitation (purple) and emission (green) spectra of **P2** in MeOH.

Quantum-mechanical calculations

N2.

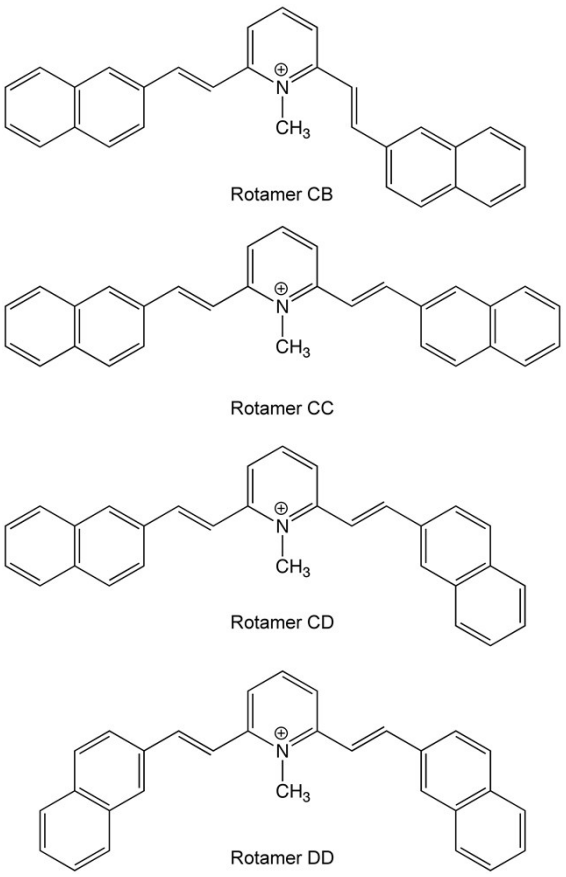

Chart S2. N2 conformers generated by rotation about the quasi-single bonds between the double bonds and the side naphthene rings or the central methyl-pyridinium unit.

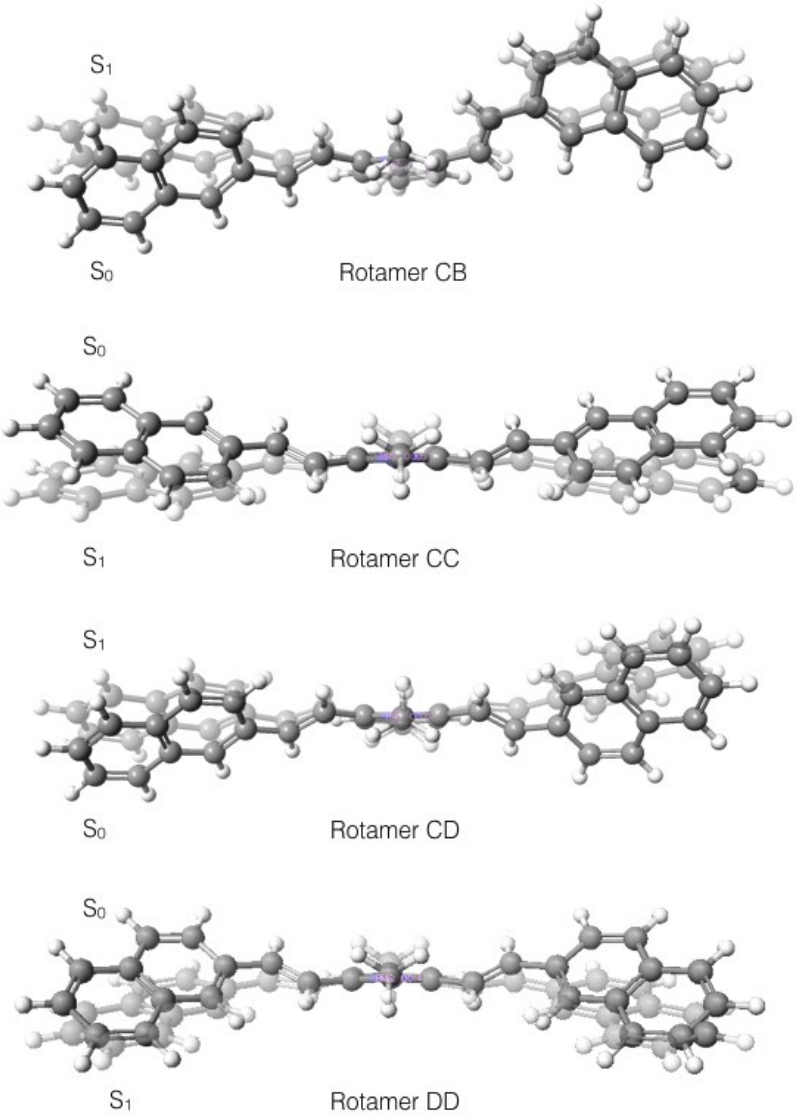

Figure S8. Molecular structures of ground and lowest excited singlet states (generally less planar and more planar, respectively) of **N2** rotamers obtained by the CAM-B3LYP/6-31G(d) model in DCM (CPCM).

Table S3. Dipole moments of **N2** rotamers together with the dihedral angles (Deg) obtained by the CAM-B3LYP/6-31G(d) model in DCM (CPCM).

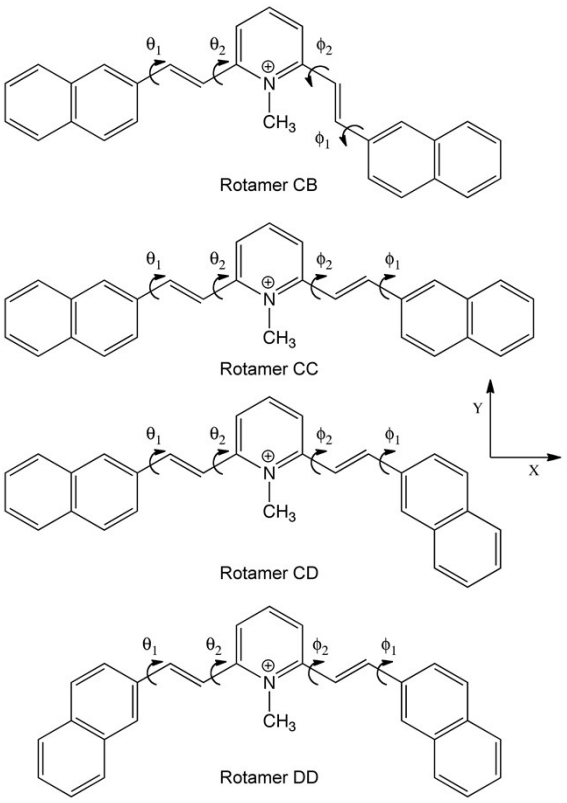

rotamer	state	$\|\mu_x\|$	$\|\mu_y\|$	$\|\mu_z\|$	$\|\mu_T\|$	θ_1	θ_2	ϕ_1	ϕ_2
CB	S_0	0.06	4.86	0.70	4.91	4.1	33.7	13.4	41.0
	$S_{1,FC}$	0.51	1.82	0.02	1.89				
	$S_{1,rel}$	2.03	2.59	0.55	3.33	1.52	15.4	6.0	17.5
	$S_0@S_{1,rel}$	0.22	4.66	0.79	4.73				
CC	S_0	0.00	3.00	1.60	3.40	2.7	34.6	2.7	34.6
	$S_{1,FC}$	0.00	0.93	0.54	1.08				
	$S_{1,rel}$	0.00	1.68	0.41	1.73	1.5	16.3	1.5	16.3
	$S_0@S_{1,rel}$	0.00	3.02	0.72	3.10				
CD	S_0	0.08	3.79	1.30	4.00	2.6	34.6	12.7	34.8
	$S_{1,FC}$	0.59	1.07	0.51	1.33				
	$S_{1,rel}$	4.68	1.65	0.30	4.97	1.2	25.4	2.1	11.1
	$S_0@S_{1,rel}$	1.99	3.72	0.45	4.25				
DD	S_0	0.00	4.68	1.10	4.80	11.3	34.2	11.5	34.3
	$S_{1,FC}$	0.02	1.29	0.49	1.38				
	$S_{1,rel}$	0.05	2.18	0.31	2.21	2.4	17.2	2.4	17.3
	$S_0@S_{1,rel}$	0.02	4.69	0.58	4.73				

Table S4. Theoretical absorption and emission wavelengths of **N2** (rotamer CC), oscillator strengths, nature and composition in terms of molecular orbitals obtained by the CAM-B3LYP/6-31G(d) model in DCM (CPCM), together with the experimental absorption and emission maxima.

Transition	λ_{th}/nm	f	MO	$c_i^2/\%$	λ_{exp}/nm
$S_0 \rightarrow S_1$	380	2.2545	$\pi_H \rightarrow \pi_L^*$	73	417
$S_0 \rightarrow S_2$	331	0.1252	$\pi_{H-1} \rightarrow \pi_L^*$	54	
$S_0 \rightarrow S_3$	305	0.0184	$\pi_{H-2} \rightarrow \pi_L^*$	49	
$S_0 \rightarrow S_4$	298	0.1152	$\pi_{H-3} \rightarrow \pi_L^*$	38	
$S_0 \rightarrow S_5$	276	0.0130	$\pi_H \rightarrow \pi_{L+1}^*$	47	
$S_0 \rightarrow S_6$	272	0.1773	$\pi_{H-1} \rightarrow \pi_{L+1}^*$	27	
$S_0 \rightarrow S_7$	260	0.3688	$\pi_H \rightarrow \pi_{L+3}^*$	42	
$S_0 \rightarrow S_8$	257	0.4641	$\pi_{H-1} \rightarrow \pi_{L+3}^*$	22	
$S_0 \rightarrow S_9$	244	0.3431	$\pi_{H-3} \rightarrow \pi_{L+1}^*$	16	
$S_0 \rightarrow S_{10}$	242	0.0112	$\pi_{H-3} \rightarrow \pi_L^*$	31	
$S_1 \rightarrow S_0$	471	2.4905	$\pi_H \rightarrow \pi_L^*$	85	505

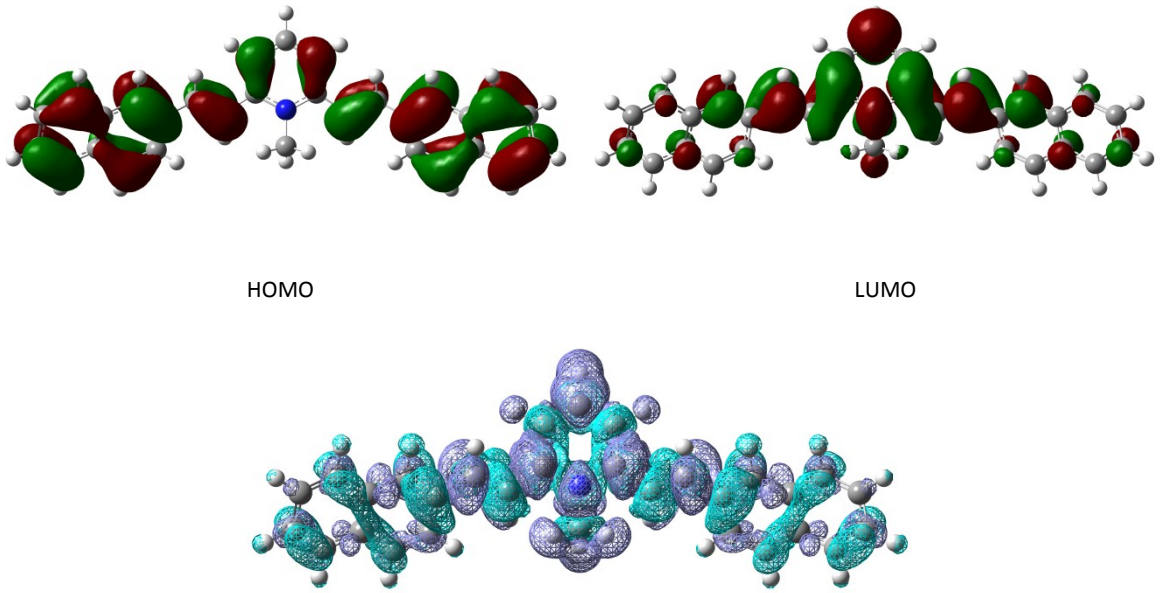

HOMO LUMO

Figure S9. Isodensity plots of **N2** (rotamer CC) obtained by the CAM-B3LYP/6-31G(d) model (upper panel). Effect of the $S_0 \rightarrow S_1$ transition on the electron density; increase and decrease of electron densities are represented by violet and cyano, respectively (lower panel).

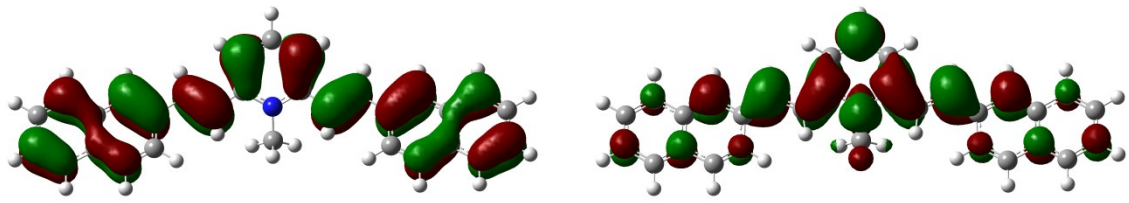

HOMO LUMO

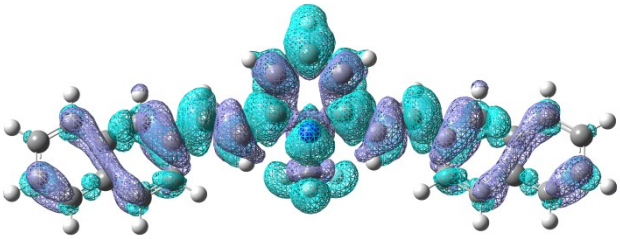

Figure S10. Isodensity plots of **N2** (rotamer CC) @$S_{1,rel}$ obtained by the CAM-B3LYP/6-31G(d) model (upper panel). Effect of the $S_1 \rightarrow S_0$ transition on the electron density @$S_{1,rel}$; increase and decrease of electron densities are represented by violet and cyano, respectively (lower panel).

Table S5. Theoretical absorption and emission wavelengths of **N2** (rotamer CD), oscillator strengths, nature and composition in terms of molecular orbitals obtained by the CAM-B3LYP/6-31G(d) model in DCM (CPCM).

Transition	λ_{th}/nm	f	MO	c_i^2/%
$S_0 \rightarrow S_1$	382	1.9820	$\pi_H \rightarrow \pi_L^*$	71
$S_0 \rightarrow S_2$	336	0.2225	$\pi_{H-1} \rightarrow \pi_L^*$	54
$S_0 \rightarrow S_3$	307	0.1266	$\pi_{H-2} \rightarrow \pi_L^*$	47
$S_0 \rightarrow S_4$	299	0.1141	$\pi_{H-3} \rightarrow \pi_L^*$	35
$S_0 \rightarrow S_5$	277	0.0290	$\pi_H \rightarrow \pi_{L+1}^*$	42
$S_0 \rightarrow S_6$	275	0.1439	$\pi_{H-1} \rightarrow \pi_{L+1}^*$	25
$S_0 \rightarrow S_7$	260	0.1524	$\pi_H \rightarrow \pi_{L+3}^*$	39
$S_0 \rightarrow S_8$	256	0.5714	$\pi_{H-1} \rightarrow \pi_{L+1}^*$	19
$S_0 \rightarrow S_9$	245	0.3625	$\pi_{H-3} \rightarrow \pi_{L+1}^*$	17
$S_0 \rightarrow S_{10}$	242	0.0402	$\pi_{H-3} \rightarrow \pi_L^*$	32
$S_1 \rightarrow S_0$	481	1.9148	$\pi_H \rightarrow \pi_L^*$	85

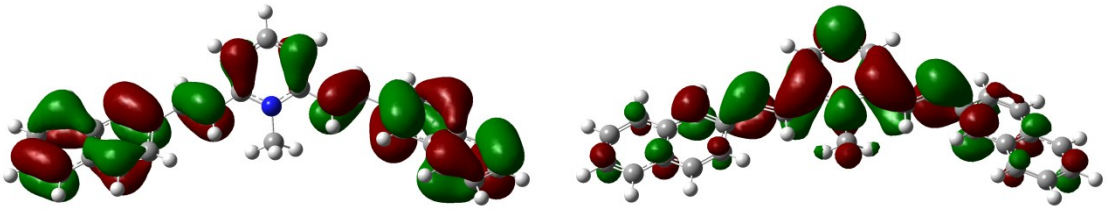

HOMO LUMO

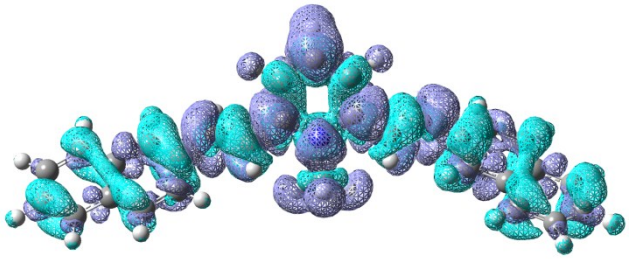

Figure S11. Isodensity plots of **N2** (rotamer CD) obtained by the CAM-B3LYP/6-31G(d) model (upper panel). Effect of the $S_0 \rightarrow S_1$ transition on the electron density; increase and decrease of electron densities are represented by violet and cyano, respectively (lower panel).

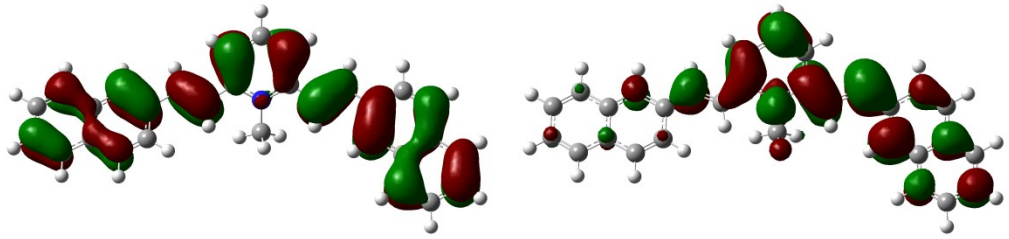

HOMO LUMO

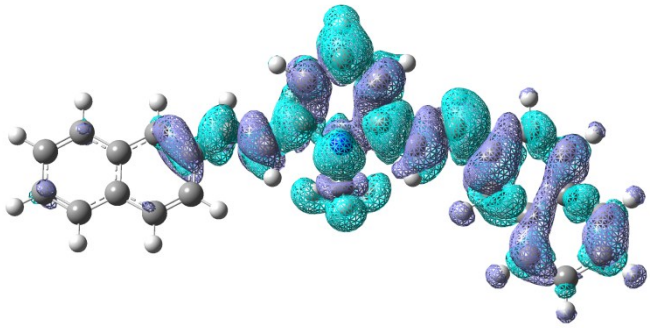

Figure S12. Isodensity plots of **N2** (rotamer CD) @$S_{1,rel}$ obtained by the CAM-B3LYP/6-31G(d) model (upper panel). Effect of the $S_1 \rightarrow S_0$ transition on the electron density @$S_{1,rel}$; increase and decrease of electron densities are represented by violet and cyano, respectively (lower panel).

Table S6. Theoretical absorption and emission wavelengths of **N2** (rotamer DD), oscillator strengths, nature and composition in terms of molecular orbitals obtained by the CAM-B3LYP/6-31G(d) model in DCM (CPCM), together with the experimental emission maximum.

Transition	λ_{th}/nm	f	MO	$c_i^2/\%$	λ_{exp}/nm
$S_0 \rightarrow S_1$	385	1.6678	$\pi_H \rightarrow \pi_L^*$	71	-
$S_0 \rightarrow S_2$	340	0.4234	$\pi_{H-1} \rightarrow \pi_L^*$	55	
$S_0 \rightarrow S_3$	310	0.2223	$\pi_{H-2} \rightarrow \pi_L^*$	49	
$S_0 \rightarrow S_4$	302	0.0942	$\pi_{H-3} \rightarrow \pi_L^*$	35	
$S_0 \rightarrow S_5$	279	0.0347	$\pi_H \rightarrow \pi_{L+1}^*$	45	
$S_0 \rightarrow S_6$	278	0.00172	$\pi_{H-1} \rightarrow \pi_{L+1}^*$	26	
$S_0 \rightarrow S_7$	261	0.0984	$\pi_H \rightarrow \pi_{L+3}^*$	41	
$S_0 \rightarrow S_8$	257	0.5674	$\pi_{H-1} \rightarrow \pi_{L+1}^*$	22	
$S_0 \rightarrow S_9$	246	0.4713	$\pi_{H-3} \rightarrow \pi_{L+1}^*$	19	
$S_0 \rightarrow S_{10}$	243	0.0079	$\pi_{H-2} \rightarrow \pi_{L+1}^*$	18	
$S_1 \rightarrow S_0$	478	1.8049	$\pi_H \rightarrow \pi_L^*$	84	450 (EPA, 77 K)

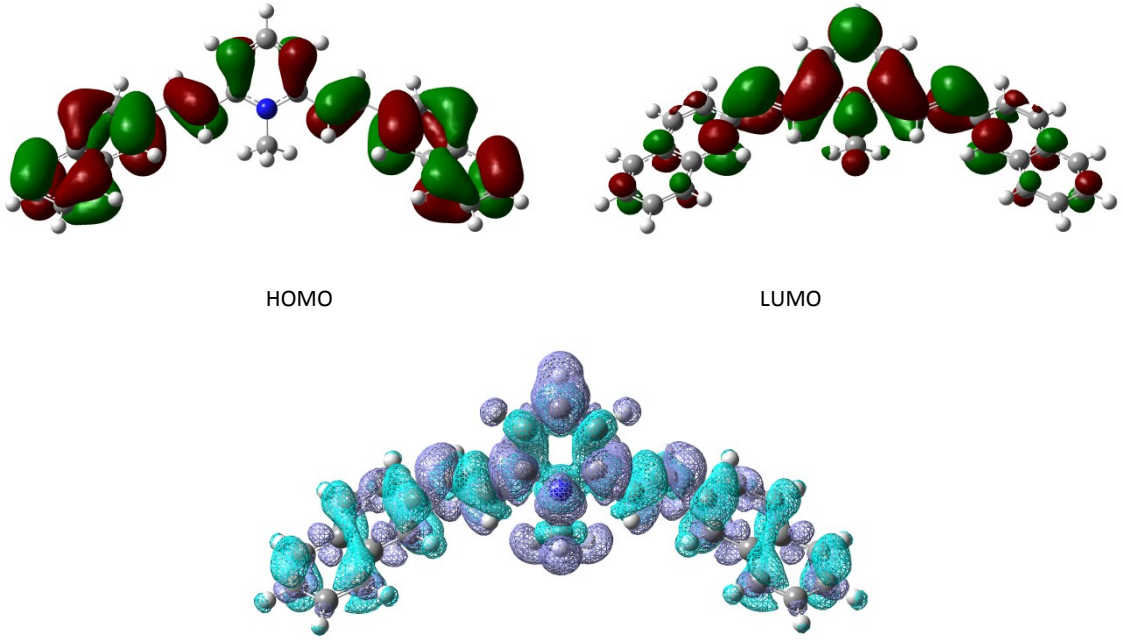

Figure S13. Isodensity plots of **N2** (rotamer DD) obtained by the CAM-B3LYP/6-31G(d) model (upper panel). Effect of the $S_0 \rightarrow S_1$ transition on the electron density; increase and decrease of electron densities are represented by violet and cyano, respectively (lower panel).

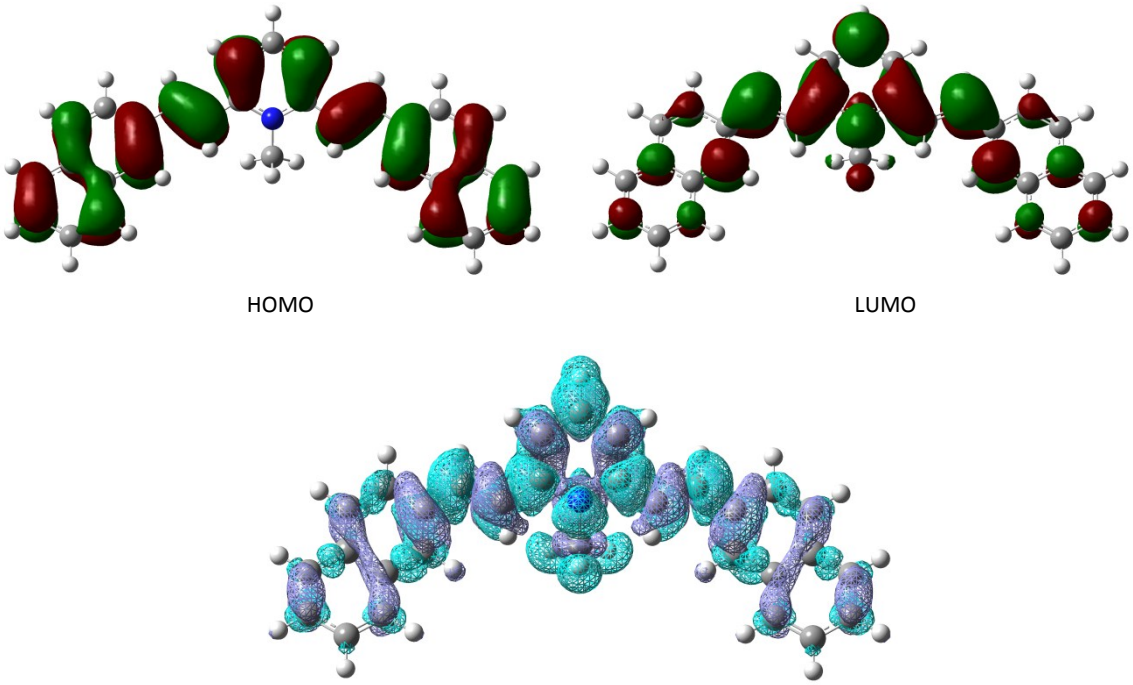

Figure S14. Isodensity plots of **N2** (rotamer DD) @$S_{1,rel}$ obtained by the CAM-B3LYP/6-31G(d) model (upper panel). Effect of the $S_1 \rightarrow S_0$ transition on the electron density @$S_{1,rel}$; increase and decrease of electron densities are represented by violet and cyano, respectively (lower panel).

Table S7. Theoretical absorption and emission wavelengths of **N2** (rotamer CB), oscillator strengths, nature and composition in terms of molecular orbitals obtained by the CAM-B3LYP/6-31G(d) model in DCM (CPCM).

Transition	**λ_{th}/nm**	**f**	**MO**	$c_i^2/\%$

$S_0 \rightarrow S_1$	385	1.9260	$\pi_H \rightarrow \pi_L^*$	72
$S_0 \rightarrow S_2$	335	0.1688	$\pi_{H-1} \rightarrow \pi_L^*$	54
$S_0 \rightarrow S_3$	307	0.0409	$\pi_{H-2} \rightarrow \pi_L^*$	48
$S_0 \rightarrow S_4$	299	0.0942	$\pi_{H-3} \rightarrow \pi_L^*$	35
$S_0 \rightarrow S_5$	278	0.1995	$\pi_H \rightarrow \pi_{L+1}^*$	43
$S_0 \rightarrow S_6$	275	0.1200	$\pi_H \rightarrow \pi_{L+2}^*$	25
$S_0 \rightarrow S_7$	261	0.4482	$\pi_H \rightarrow \pi_{L+3}^*$	39
$S_0 \rightarrow S_8$	257	0.3938	$\pi_{H-1} \rightarrow \pi_{L+1}^*$	21
$S_0 \rightarrow S_9$	245	0.3400	$\pi_{H-3} \rightarrow \pi_{L+1}^*$	18
$S_0 \rightarrow S_{10}$	243	0.0281	$\pi_{H-3} \rightarrow \pi_L^*$	32
$S_1 \rightarrow S_0$	494	1.9767	$\pi_H \rightarrow \pi_L^*$	86

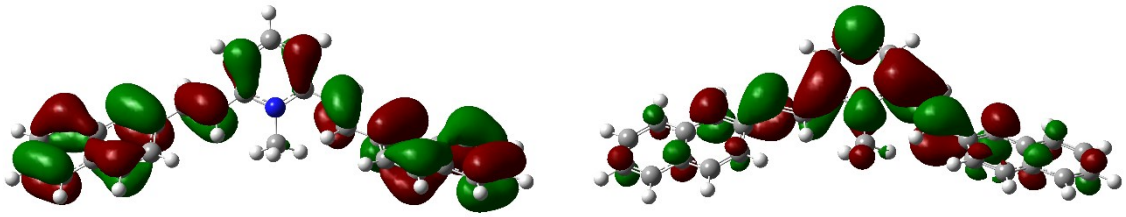

HOMO LUMO

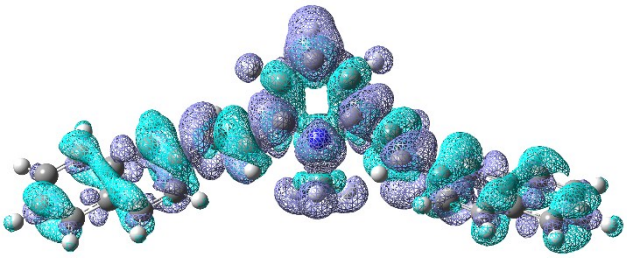

Figure S15. Isodensity plots of **N2** (rotamer CB) obtained by the CAM-B3LYP/6-31G(d) model (upper panel). Effect of the $S_0 \rightarrow S_1$ transition on the electron density; increase and decrease of electron densities are represented by violet and cyano, respectively (lower panel).

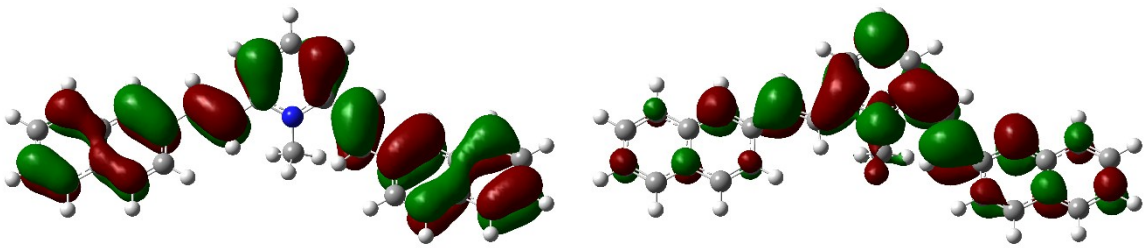

HOMO LUMO

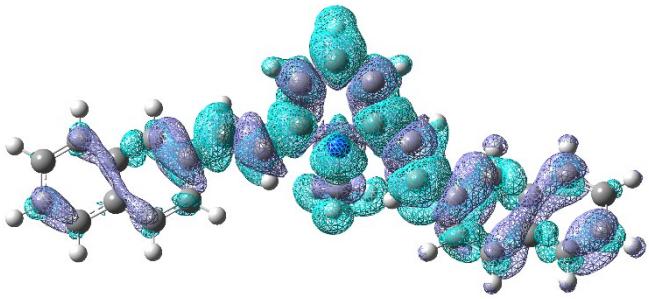

Figure S16. Isodensity plots of **N2** (rotamer CB) @$S_{1,rel}$ obtained by the CAM-B3LYP/6-31G(d) model (upper panel). Effect of the $S_1 \rightarrow S_0$ transition on the electron density @$S_{1,rel}$; increase and decrease of electron densities are represented by violet and cyano, respectively (lower panel).

P2.

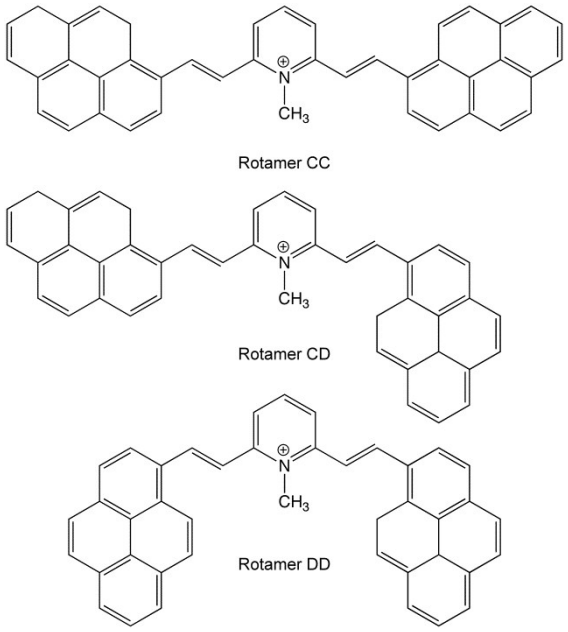

Chart S3. P2 conformers generated by rotation about the quasi-single bonds between the double bonds and the side pyrene rings or the central methyl-pyridinium unit.

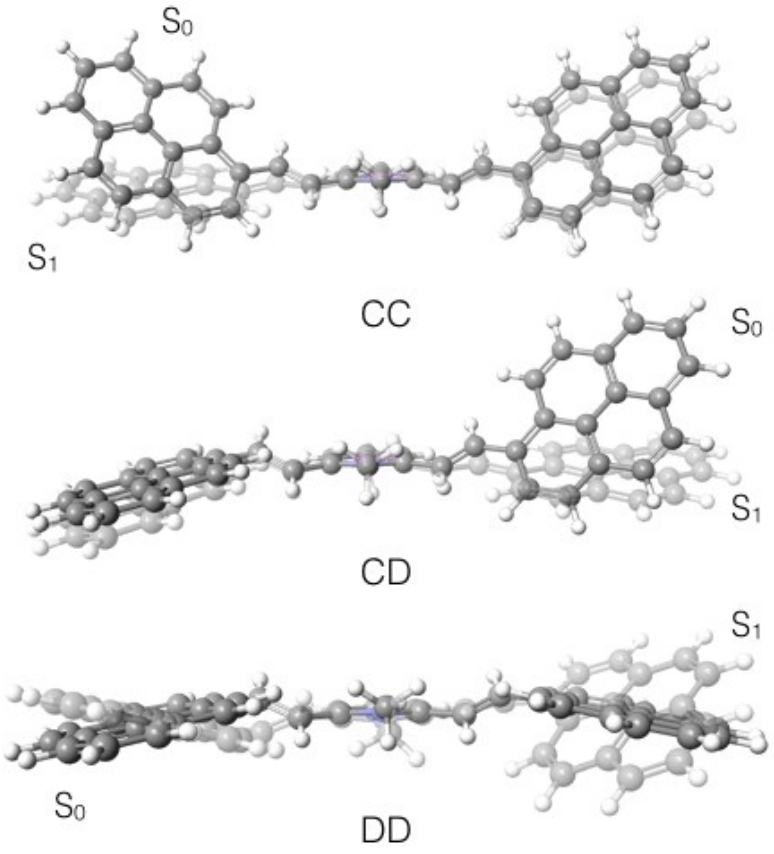

Figure S17. Molecular structures of ground and lowest excited singlet states (generally less planar and more planar, respectively) of **P2** rotamers obtained by the CAM-B3LYP/6-31G(d) model in DCM (CPCM).

Table S8. Dipole moments of **P2** rotamers together with the dihedral angles (Deg) obtained by the CAM-B3LYP/6-31G(d) model in DCM (CPCM).

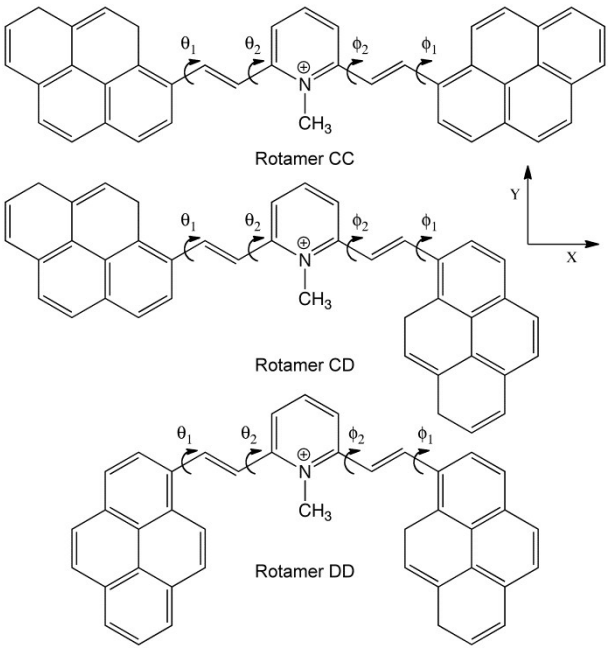

rotamer	state	$\lvert\mu_x\rvert$	$\lvert\mu_y\rvert$	$\lvert\mu_z\rvert$	$\lvert\mu_T\rvert$	θ_1	θ_2	ϕ_1	ϕ_2
CC	S_0	0.00	3.84	2.35	4.50	26.4	34.1	26.4	34.1
	$S_{1,FC}$	0.01	1.07	0.88	1.39				
	$S_{1,rel}$	10.9	0.61	0.43	10.9	1.3	9.7	21.4	32.6
	$S_0@S_{1,rel}$	4.6	1.20	1.14	4.88				
CD	S_0	0.61	6.04	2.03	6.41	27.8	36.1	34.1	32.6
	$S_{1,FC}$	0.55	1.62	0.68	1.84				
	$S_{1,rel}$	10.8	2.08	0.22	11.0	1.3	9.2	31.3	33.0
	$S_0@S_{1,rel}$	4.27	4.00	0.38	5.87				
DD	S_0	0.00	8.60	0.26	8.60	33.6	33.9	33.9	33.6
	$S_{1,FC}$	0.00	2.33	0.22	2.34				
	$S_{1,rel}$	9.75	2.65	0.60	10.1	20.1	4.8	33.7	34.1
	$S_0@S_{1,rel}$	4.54	6.63	0.65	8.06				

Table S9. Theoretical absorption and emission wavelengths of **P2** (rotamer CC), oscillator strengths, nature and composition in terms of molecular orbitals obtained by the CAM-B3LYP/6-31G(d) model in DCM (CPCM), together with the experimental absorption and emission maxima.

Transition	λ_{th}/nm	f	MO	$c_i^2/_{\%}$	λ_{exp}/nm
$S_0 \rightarrow S_1$	439	2.3292	$\pi_H \rightarrow \pi_L^*$	71	496
$S_0 \rightarrow S_2$	399	0.3477	$\pi_{H-1} \rightarrow \pi_L^*$	59	
$S_0 \rightarrow S_3$	328	0.0030	$\pi_{H-2} \rightarrow \pi_L^*$	32	
$S_0 \rightarrow S_4$	324	0.0212	$\pi_{H-3} \rightarrow \pi_L^*$	26	
$S_0 \rightarrow S_5$	319	0.1311	$\pi_{H-1} \rightarrow \pi_{L+1}^*$	25	
$S_0 \rightarrow S_6$	316	0.1079	$\pi_H \rightarrow \pi_{L+1}^*$	40	
$S_0 \rightarrow S_7$	290	0.6569	$\pi_H \rightarrow \pi_{L+3}^*$	38	
$S_0 \rightarrow S_8$	286	0.2289	$\pi_{H-1} \rightarrow \pi_{L+1}^*$	19	
$S_0 \rightarrow S_9$	278	0.1047	$\pi_{H-4} \rightarrow \pi_L^*$	27	
$S_0 \rightarrow S_{10}$	269	0.1432	$\pi_{H-3} \rightarrow \pi_L^*$	24	
$S_1 \rightarrow S_0$	572	2.3814	$\pi_H \rightarrow \pi_L^*$	81	615

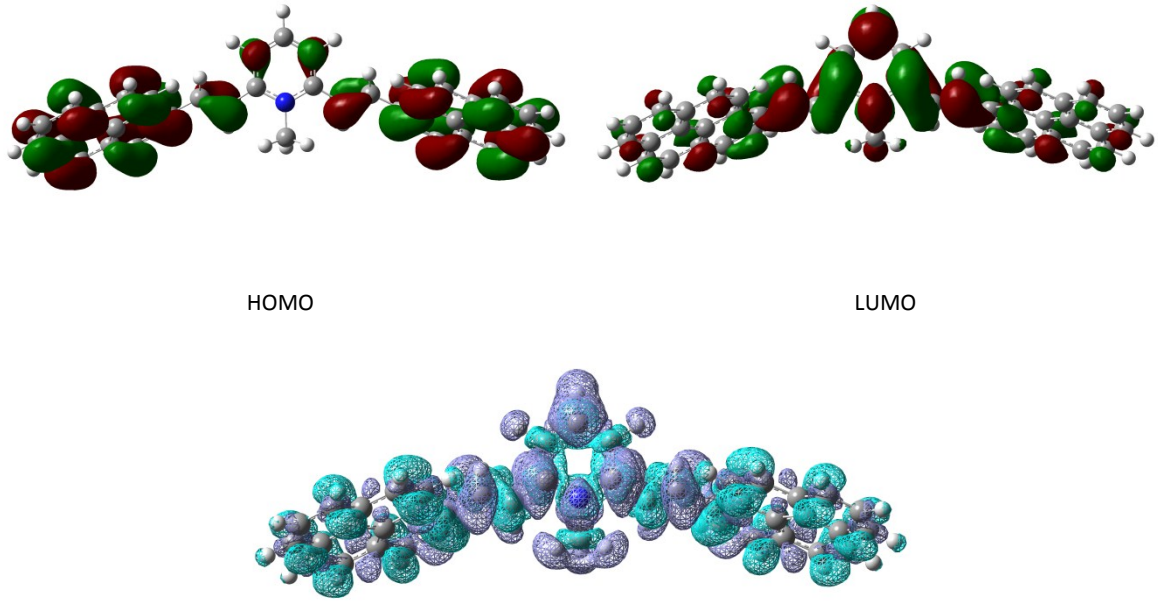

Figure S18. Isodensity plots of **P2** (rotamer CC) obtained by the CAM-B3LYP/6-31G(d) model (upper panel). Effect of the $S_0 \rightarrow S_1$ transition on the electron density; increase and decrease of electron densities are represented by violet and cyano, respectively (lower panel).

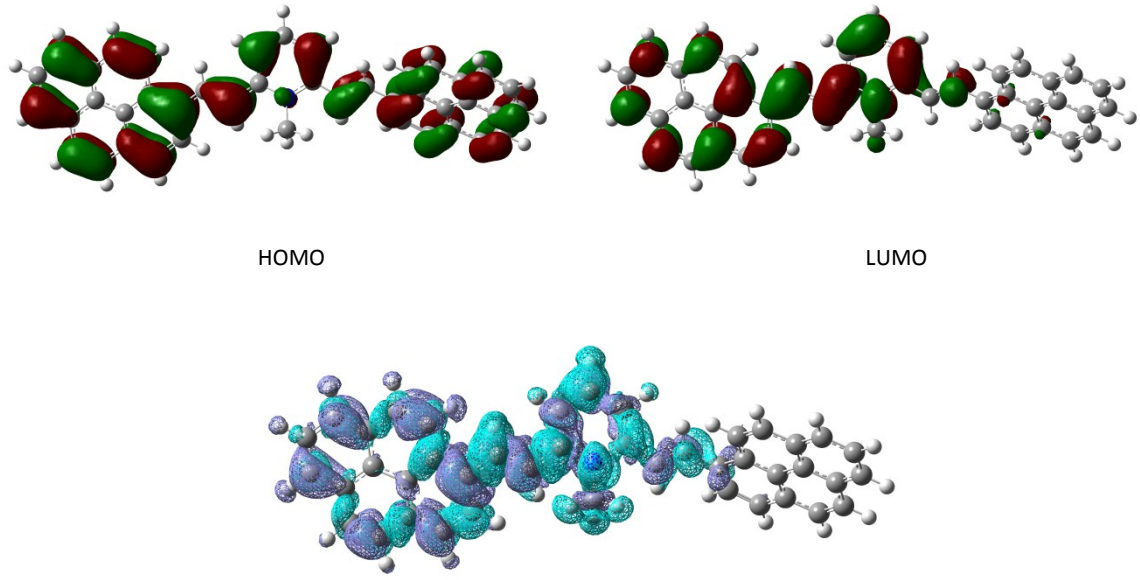

Figure S19. Isodensity plots of **P2** (rotamer CC) @$S_{1,rel}$ obtained by the CAM-B3LYP/6-31G(d) model (upper panel). Effect of the $S_1 \rightarrow S_0$ transition on the electron density; increase and decrease of electron densities are represented by violet and cyano, respectively (lower panel).

Table S10. Theoretical absorption and emission wavelengths of **P2** (rotamer CD), oscillator strengths, nature and composition in terms of molecular orbitals obtained by the CAM-B3LYP/6-31G(d) model in DCM (CPCM).

Transition	λ_{th}/nm	f	MO	c_i^2/%
$S_0 \rightarrow S_1$	431	1.9372	$\pi_H \rightarrow \pi_L^*$	71
$S_0 \rightarrow S_2$	395	0.4834	$\pi_{H-1} \rightarrow \pi_L^*$	60
$S_0 \rightarrow S_3$	326	0.1847	$\pi_{H-2} \rightarrow \pi_L^*$	33
$S_0 \rightarrow S_4$	323	0.0133	$\pi_{H-3} \rightarrow \pi_L^*$	25
$S_0 \rightarrow S_5$	318	0.2031	$\pi_H \rightarrow \pi_{L+2}^*$	27
$S_0 \rightarrow S_6$	313	0.1231	$\pi_H \rightarrow \pi_{L+1}^*$	38
$S_0 \rightarrow S_7$	289	0.0990	$\pi_H \rightarrow \pi_{L+3}^*$	38
$S_0 \rightarrow S_8$	285	0.5276	$\pi_{H-1} \rightarrow \pi_{L+1}^*$	19
$S_0 \rightarrow S_9$	278	0.1736	$\pi_{H-1} \rightarrow \pi_{L+3}^*$	22
$S_0 \rightarrow S_{10}$	269	0.0695	$\pi_{H-3} \rightarrow \pi_L^*$	28
$S_1 \rightarrow S_0$	572	2.1690	$\pi_H \rightarrow \pi_L^*$	82

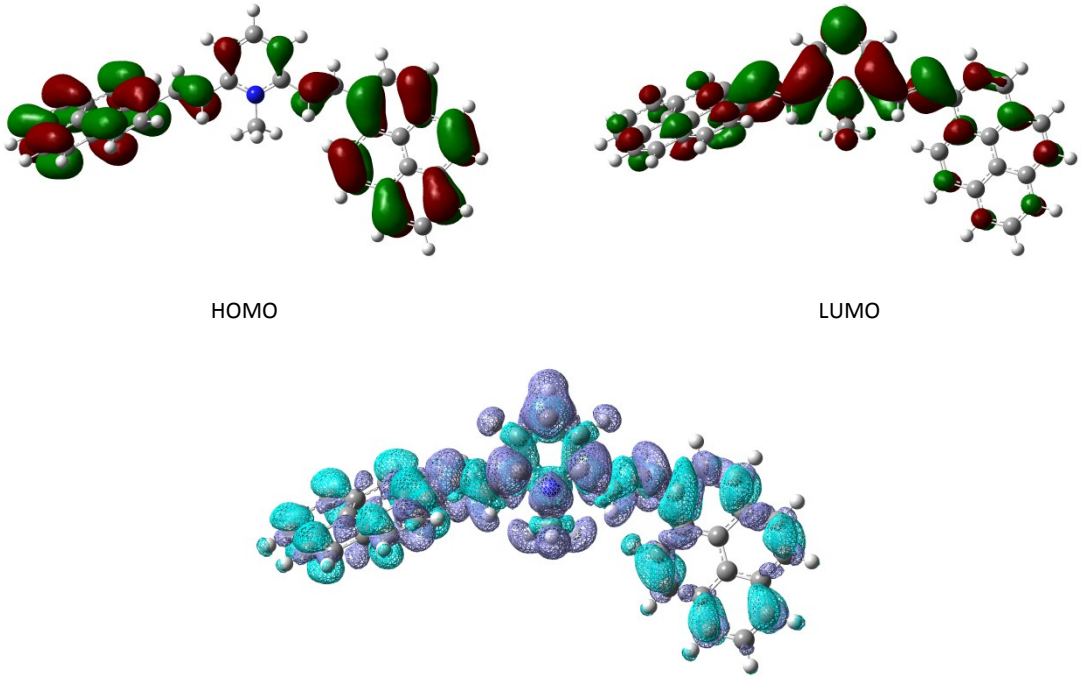

HOMO LUMO

Figure S20. Isodensity plots of **P2** (rotamer CD) obtained by the CAM-B3LYP/6-31G(d) model (upper panel). Effect of the $S_0 \rightarrow S_1$ transition on the electron density; increase and decrease of electron densities are represented by violet and cyano, respectively (lower panel).

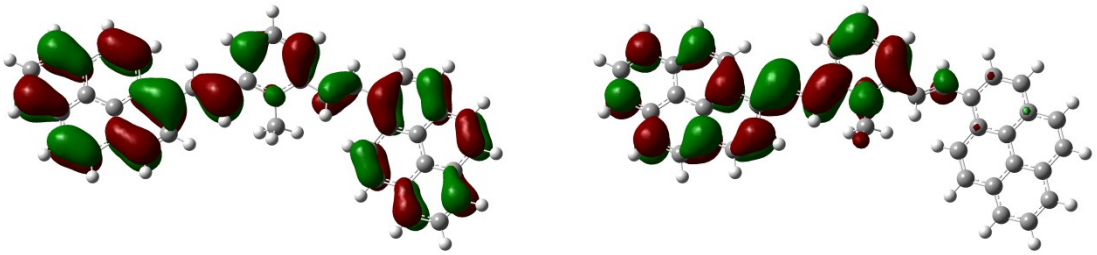

HOMO LUMO

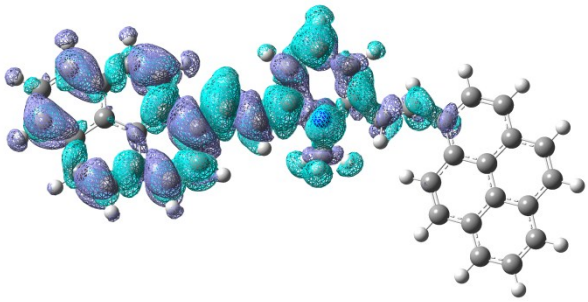

Figure S21. Isodensity plots of **P2** (rotamer CD) @$S_{1,rel}$ obtained by the CAM-B3LYP/6-31G(d) model (upper panel). Effect of the $S_1 \rightarrow S_0$ transition on the electron density; increase and decrease of electron densities are represented by violet and cyano, respectively (lower panel).

Table S11. Theoretical absorption and emission wavelengths of **P2** (rotamer DD), oscillator strengths, nature and composition in terms of molecular orbitals obtained by the CAM-B3LYP/6-31G(d) model in DCM (CPCM).

Transition	λ_{th}/nm	f	MO	c_i^2/%
$S_0 \rightarrow S_1$	429	1.3605	$\pi_H \rightarrow \pi_L^*$	72
$S_0 \rightarrow S_2$	393	0.9872	$\pi_{H-1} \rightarrow \pi_L^*$	61
$S_0 \rightarrow S_3$	325	0.1549	$\pi_{H-2} \rightarrow \pi_L^*$	34
$S_0 \rightarrow S_4$	322	0.0182	$\pi_{H-3} \rightarrow \pi_L^*$	25
$S_0 \rightarrow S_5$	317	0.0039	$\pi_H \rightarrow \pi_{L+2}^*$	30
$S_0 \rightarrow S_6$	313	0.2921	$\pi_H \rightarrow \pi_{L+1}^*$	38
$S_0 \rightarrow S_7$	288	0.1586	$\pi_H \rightarrow \pi_{L+3}^*$	41
$S_0 \rightarrow S_8$	285	0.6200	$\pi_{H-4} \rightarrow \pi_L^*$	23
$S_0 \rightarrow S_9$	279	0.0021	$\pi_{H-1} \rightarrow \pi_{L+3}^*$	29
$S_0 \rightarrow S_{10}$	270	0.0259	$\pi_{H-3} \rightarrow \pi_L^*$	33
$S_1 \rightarrow S_0$	580	1.5034	$\pi_H \rightarrow \pi_L^*$	83

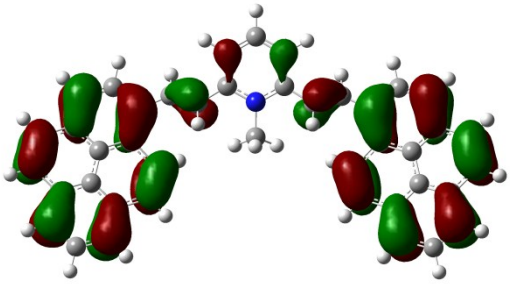

HOMO

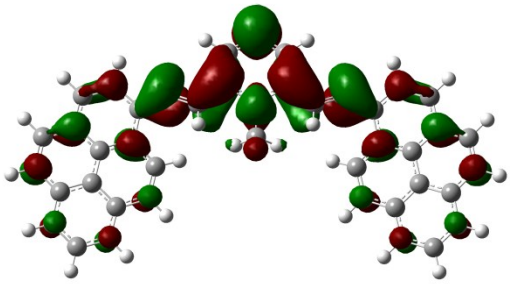

LUMO

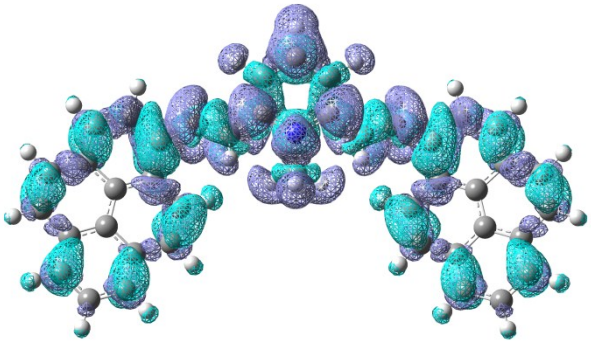

Figure S22. Isodensity plots of **P2** (rotamer DD) obtained by the CAM-B3LYP/6-31G(d) model (upper panel). Effect of the $S_0 \rightarrow S_1$ transition on the electron density; increase and decrease of electron densities are represented by violet and cyano, respectively (lower panel).

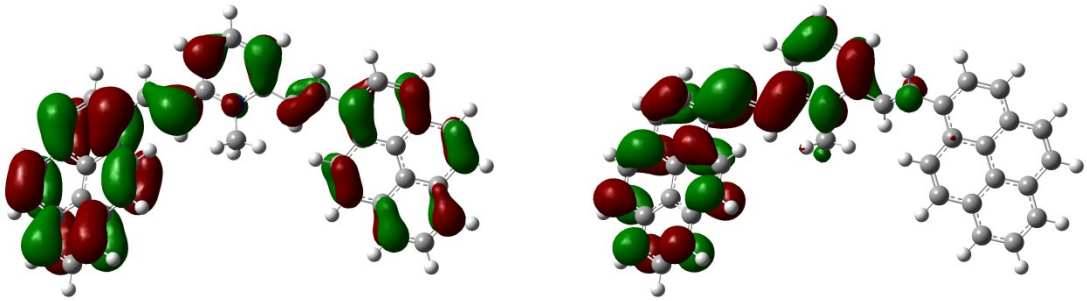

HOMO LUMO

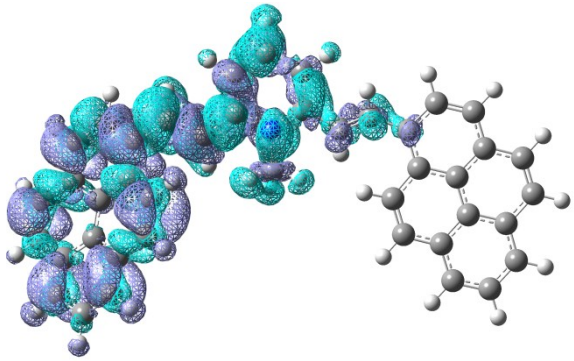

Figure S23. Isodensity plots of **P2** (rotamer DD) @$S_{1,rel}$ obtained by the CAM-B3LYP/6-31G(d) model (upper panel). Effect of the $S_1 \rightarrow S_0$ transition on the electron density; increase and decrease of electron densities are represented by violet and cyano, respectively (lower panel).

Ultrafast measurements

Table S12. Spectral and kinetic properties of **N2** obtained from femtosecond excited state absorption measurements in solvents of different polarity and/or viscosity.

Compound	Solvent	τ /ps	λ /nm	Assignment
N2	DCM	0.84	470(−), 535(+)^{sh}, 710(+)	Solv./RI
		16	460(+), 550(–), 705(+)	VC
		160	465(+), 545(−), 705(+)	$S_{1,rel}$
	DCE	0.40	<470(–), 530(+), 665(+)^{sh}	Solv.
		2.6	495(–), 540(–), 680(+)	Solv./RI
		13	540(–), 690(+)	VC
		210	540(−), 685(+)	$S_{1,rel}$
	2-PrOH	0.83	485(−), 525(+)^{sh}, 670(+)	Solv.
		5.9	495(−), 535(–)^{sh}, 680(+)	Solv./RI
		42	535(–), 680(+)	Solv.
		320	540(–), 680(+)	$S_{1,rel}$
	EtOH	0.45	<480(−), 540(+), 720(+)^{sh}	Solv.
		2.9	485(−),720(+)^{sh}	Solv./RI
		29	535(–), 720(+)^{sh}	Solv.
		310	450(+), 540(−),720(+)^{sh}	$S_{1,rel}$
	MeOH	0.13	<465(−), 540(+), 675(+)^{sh}	Solv.
		1.7	485(−), 705(+)^{sh}	Solv./RI
		11	535(–), 720(+)	Solv.
		290	540(−), 700(+)	$S_{1,rel}$
	MeCN	0.10	<475(−), 540(+)	Solv.
		0.67	485(−), 575(+)	Solv./RI
		24	455(+), 545(–), 710(+)	VC
		370	455(+), 540(−), 710(+)	$S_{1,rel}$
	MeOH/Gly 50:50	0.20	535(+), 685(+)^{sh}	Solv.
		3.4	<490(–), 540(+)^{sh}, 665(+)	Solv.
		31	495(−), 535(–)^{sh}, 670(+)	Solv./RI
		380	535(−), 675(+)	$S_{1,rel}$
	EtGly	0.20	545(+), 660(+)^{sh}	Solv.
		2.5	<490(–), 540(+)^{sh}, 665(+)	Solv.
		30	500(−), 535(–)^{sh}, 670(+)	Solv./RI
		520	540(−), 680(+)	$S_{1,rel}$
	W/EtOH 70:30	0.10	530(+)	Solv.
		1.0	485(−), 595(+)^{sh}, 720(+)^{sh}	Solv./RI
		6.9	450(+), 525(−), 715(+)	Solv.
		270	455(+), 545(–), 700(+)	$S_{1,rel}$

Solv. = solvation; **VC** = vibrational cooling; **RI** = rotamer interconversion.

Table S13. Spectral and kinetic properties of **P1** obtained from femtosecond excited state absorption measurements in solvents of different polarity and/or viscosity.

Compound	Solvent	τ /ps	λ /nm	Assignment
P1*	DCM	1.3	540(−), 620(+)	Solv./S_1 (LE)
		34	560(+), 720(−)	S_1 (TICT)
		420	545(+), 630(−)	S_1 (PICT)
	DCE	0.1	broad	Solv.
		18	550(+)	S_1 (TICT)
		160	540(+), 615(−)	S_1 (PICT)
	2-PrOH	<0.1	650(+)	Solv.
		10	600(+)	Solv./S_1 (LE)
		40	550(+), 635(−)	S_1 (TICT)
		390	540(+), 620(−)	S_1 (PICT)
	EtOH	0.83	500(−), 640(+)	Solv.
		5.2	535(−), 610(+)	Solv./S_1 (LE)
		30	580(+)	S_1 (TICT)
		285	540(+), 630(−)	S_1 (PICT)
	MeOH	0.37	550(−), 640(+)	Solv.
		2.8	535(−), 610(+)	Solv./S_1 (LE)
		29	555(+)	S_1 (TICT)
		295	535(+), 625(−)	S_1 (PICT)
	MeCN	0.15	535(−), 640(+)	Solv.
		0.84	530(−), 605(+)	Solv./S_1 (LE)
		32	545(+), 645(−)	S_1 (TICT)
		310	535(+), 625(−)	S_1 (PICT)

* From ref. 29.

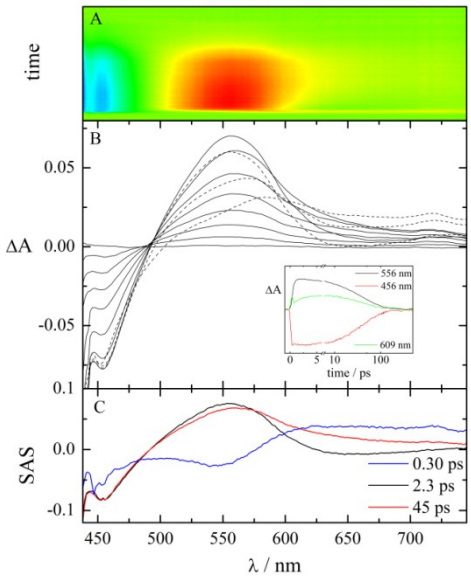

Figure S24. Pump-probe absorption spectroscopy of **P2** in MeCN (λ_{exc} = 400 nm): (A) contour plot of the experimental data, (B) time-resolved absorption spectra recorded at increasing delays after the laser pulse (inset: decay kinetics at meaningful wavelengths, with a linear scale for the first picoseconds and a *log* scale for longer times), and (C) Species Associated Spectra (SAS) calculated by Target Analysis.

Table S14. Spectral and kinetic properties of **P2** obtained from femtosecond excited state absorption measurements in solvents of different polarity and/or viscosity.

Compound	Solvent	τ /ps	λ /nm	Assignment
P2	DCM	0.71	470(−), 605(+)^{sh}, 725(+)	Solv./S_1 (LE)
		430	465(−), 570(+), 660(−)	S_1 (ICT)
		rest	575(+)	T_1
	DCE	1.4	470(−), 605(+), 690(+)^{sh}	Solv./S_1 (LE)
		300	<505(−), 565(+), 660(−)	S_1 (ICT)
		rest	570(+)	T_1
	2-PrOH	1.9	<545(−), 610(+)	Solv.
		12	<500(–), 535(+)^{sh}, 580(+), 700(+)	Solv./S_1 (LE)
		400	<500(–), 555(+), 650(−)	S_1 (ICT)
		rest	620(+)	T_1
	EtOH	2.0	455(−), 540(–)^{sh}, 595(+)	Solv./S_1 (LE)
		21	450(−), 555(+), 640(−)	Solv.
		190	450(−), 560(+), 665(−)	S_1 (ICT)
		rest	broad	T_1
	MeOH/Gly (70:30)	0.51	<535(–), 625(+)	Solv.
		7.0	525(+)^{sh}, 590(+)	Solv./S_1 (LE)
		165	555(+), 655(−)	S_1 (ICT)
	MeOH	0.67	520(−), 610(+)	Solv./S_1 (LE)
		3.9	450(−), 555(+), 640(−)	Solv.
		73	450(−), 560(+)	S_1 (ICT)
		rest	broad	T_1
	Ac	0.52	545(−), 625(+)	Solv./S_1 (LE)
		3.2	<490(−), 550(+), 650(−)	Solv./VC
		64	<490(−), 560(+)	S_1 (ICT)
		rest	broad	T_1
	MeCN	0.30	450(−), 545(−), 625(+)	Solv./S_1 (LE)
		2.3	455(−), 555(+), 655(−)	Solv./VC
		45	455(−), 560(+)	S_1 (ICT)
	EtGly	0.61	<525(−), 650(+)	Solv.
		2.9	<500(−), 630(+)	Solv.
		20	<485(–), 530(+)^{sh}, 585(+)	Solv./S_1 (LE)
		170	<485(–), 550(+), 700(−)	S_1 (ICT)
		rest	620(+)	T_1

Temperature and viscosity effect on absorption and emission

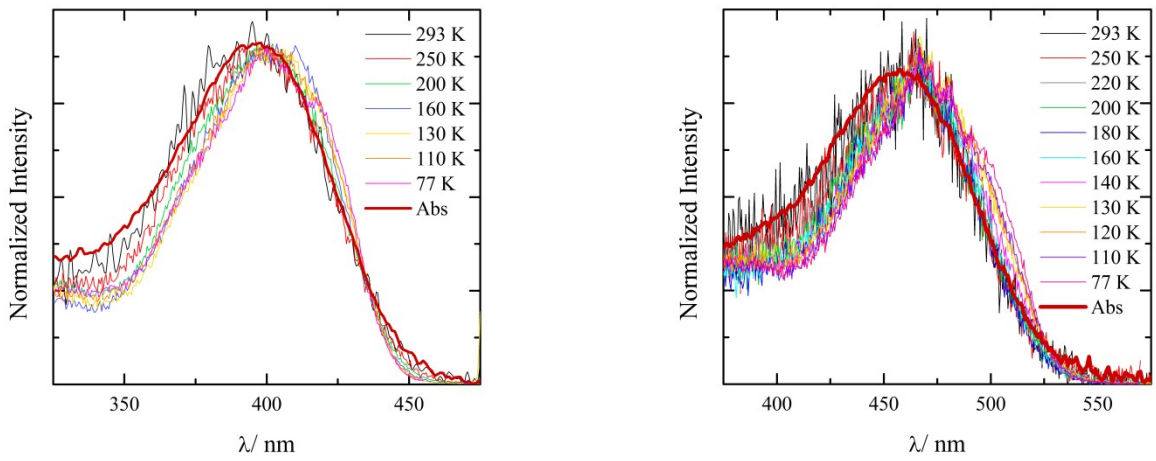

Figure S25. Temperature effect on the excitation spectra of **N2**, left graph, and **P2**, right graph, in EPA. The absorption spectrum recorded at room temperature is reported in red solid line for comparison purposes.

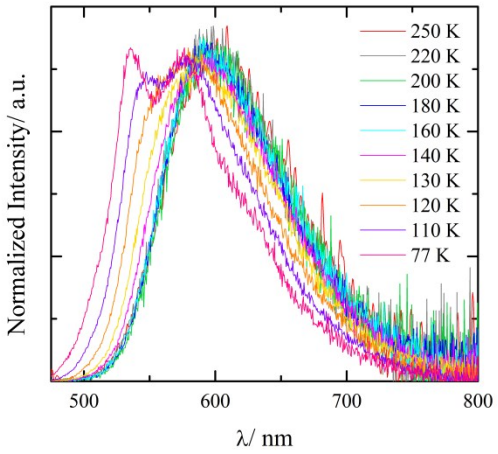

Figure S26. Area normalized emission spectra (λ_{exc} = 465 nm) of **P2** in EPA as a function of temperature.

Table S15. Fluorescence quantum yields (ϕ_F) of **N2**in EPA at different temperatures (λ_{exc}= 397 nm).

T /K	ϕ_F
293	0.032
250	0.15
200	0.38
160	0.47
130	0.43
110	0.39
77	0.45

Table S16. Fluorescence quantum yields (ϕ_F) of **P2** in EPA at different temperatures (λ_{exc}= 465 nm).

T /K	ϕ_F
293	0.037
250	0.081
220	0.11
200	0.20
180	0.26
160	0.34
140	0.45
130	0.55
120	0.69
110	0.85
77	0.94

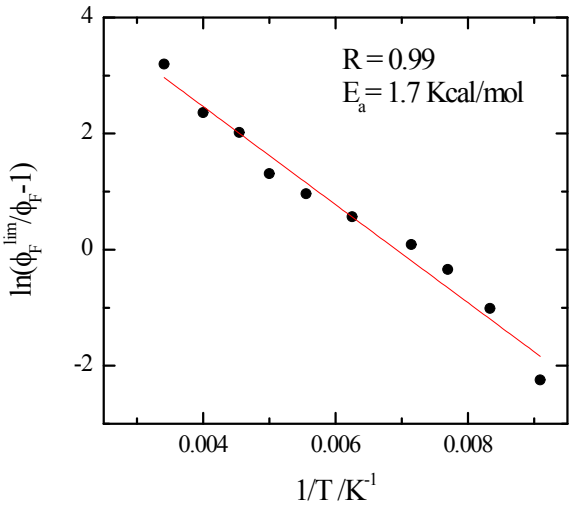

Figure S27. Plot of the fluorescence quantum yields according to the Arrhenius-type equation.